Human Brain Mapping

WILEY

RESEARCH ARTICLE OPEN ACCESS

TR(Acking) Individuals Down: Exploring the Effect of Temporal Resolution in Resting-State Functional MRI Fingerprinting

Barbara Cassone[1,2] | Francesca Saviola[1,3] | Stefano Tambalo[1,4,5] | Enrico Amico[3,6,7,8] | Sebastian Hübner[1] | Silvio Sarubbo[9,10] | Dimitri Van De Ville[3,6] | Jorge Jovicich[1]

[1]CIMeC, Center for Mind/Brain Sciences, University of Trento, Rovereto, Trento, Italy | [2]Department of Psychology, University of Milano-Bicocca, Milan, Italy | [3]Neuro-X Institute, Ecole Polytechnique Fédérale de Lausanne, Geneva, Switzerland | [4]Department of Physics, University of Torino, Torino, Italy | [5]Department of Molecular Biotechnology and Health Sciences, University of Trento, Torino, Italy | [6]Department of Radiology and Medical Informatics, University of Geneva, Geneva, Switzerland | [7]School of Mathematics, University of Birmingham, Birmingham, UK | [8]Centre for Human Brain Health, University of Birmingham, Birmingham, UK | [9]Department of Physics, University of Torino, Torino, Italy | [10]Department of Molecular Biotechnology and Health Sciences, University of Torino, Torino, Italy

Correspondence: Jorge Jovicich (jorge.jovicich@unitn.it)

Received: 3 April 2024 | **Revised:** 6 November 2024 | **Accepted:** 20 December 2024

Funding: This work was supported by ISMRM Exchange Award, Provincia Autonoma di Trento, Ministero dell'Istruzione, dell'Università e della Ricerca, Swiss National Science Foundation, Ambizione project, PZ00P2_185716, and Municipality of the City of Rovereto.

Keywords: brain fingerprinting | brain networks | functional connectivity | resting-state fMRI | temporal resolution

ABSTRACT

Functional brain fingerprinting has emerged as an influential tool to quantify reliability in neuroimaging studies and to identify cognitive biomarkers in both healthy and clinical populations. Recent studies have revealed that brain fingerprints reside in the timescale-specific functional connectivity of particular brain regions. However, the impact of the acquisition's temporal resolution on fingerprinting remains unclear. In this study, we examine for the first time the reliability of functional fingerprinting derived from resting-state functional MRI (rs-fMRI) with different whole-brain temporal resolutions (TR = 0.5, 0.7, 1, 2, and 3 s) in a cohort of 20 healthy volunteers. Our findings indicate that subject identifiability within a fixed TR is successful across different temporal resolutions, with the highest identifiability observed at TR 0.5 and 3 s (TR(s)/identifiability(%): 0.5/64; 0.7/47; 1/44; 2/44; 3/56). We discuss this observation in terms of protocol-specific effects of physiological noise aliasing. We further show that, irrespective of TR, associative brain areas make an higher contribution to subject identifiability (functional connections with highest mean ICC: within subcortical network [SUB; ICC = 0.0387], within default mode network [DMN; ICC = 0.0058]; between DMN and somato-motor [SM] network [ICC = 0.0013]; between ventral attention network [VA] and DMN [ICC = 0.0008]; between VA and SM [ICC = 0.0007]), whereas sensory-motor regions become more influential when integrating data from different TRs (functional connections with highest mean ICC: within fronto-parietal network [ICC = 0.382], within dorsal attention network [DA; ICC = 0.373]; within SUB [ICC = 0.367]; between visual network [VIS] and DA [ICC = 0.362]; within VIS [ICC = 0.358]). We conclude that functional connectivity fingerprinting derived from rs-fMRI holds significant potential for multicentric studies also employing protocols with different temporal resolutions. However, it remains crucial to consider fMRI signal's sampling rate differences in subject identifiability between data samples, in order to improve reliability and generalizability of both whole-brain and specific functional networks' results. These findings contribute to a better understanding of the practical application of functional connectivity fingerprinting, and its implications for future neuroimaging research.

Summary

- Intrinsic functional brain activity fingerprints have valuable applications in both basic neuroscientific research and precision medicine.
- Reproducibility of functional fingerprints is robust across various temporal resolutions, with higher subject identifiability at TR 0.5 and 3 s.
- Associative brain areas (fronto-parietal, default mode and attention networks) mostly contribute to subject identifiability regardless of TR, while sensory-motor regions are more sensible to differences in temporal resolution.

1 | Introduction

In recent years, brain connectome fingerprinting has shown increased promise as a tool for understanding underlying mechanisms of the human brain, in particular those related to functional connectivity (FC), which represents the statistical interdependency between brain regions' activity across time (Friston 1994). In their seminal work, Finn et al. (2015) were among the first to show that an individual's FC profile is not only unique, but also reliable enough to be identified and distinguished with high accuracy from a larger sample of similar healthy individuals. Following studies expanded on the topic by showing that functional patterns are useful to detect subject-level biomarkers of behavioral outcome and cognitive performance (Amico and Goñi 2018; Romano et al. 2022; Sorrentino et al. 2021; Svaldi et al. 2021; Troisi Lopez et al. 2023), opening up the possibility to predict clinical scores and contributing to personalized treatments planning (Castellanos et al. 2013; Fernandes et al. 2017; Smith et al. 2015) and biometric systems (Fraschini et al. 2015; Rocca et al. 2014).

Another relevant application of the study of brain fingerprints relates to one essential aspect and source of concern for numerous domains of scientific research (Begley and Ioannidis 2015), that is reproducibility and generalizability of results. In particular, Amico and Goñi (2018) introduced the "identifiability framework" for assessing and increasing subject identification across visits, by running principal component analysis (PCA) on a group's functional connectomes, and removing "noise" components while retaining only components necessary for subject identification. This procedure has been shown to increase test–retest reliability across different tasks (Amico and Goñi 2018; Rajapandian et al. 2020), scanning lengths (Amico and Goñi 2018), magnetic resonance imaging (MRI) scanners and sites (Bari et al. 2019), network properties (Rajapandian et al. 2020), imaging modalities, namely functional magnetic resonance imaging (fMRI) and magnetoencephalography, FC measures and frequency bands (Sareen et al. 2021). Moreover, specific brain regions have been found to give a different contribution to fingerprinting (Amico and Goñi 2018; Romano et al. 2022; Sorrentino et al. 2021; Svaldi et al. 2021; Troisi Lopez et al. 2023; Van De Ville et al. 2021), which is maximized at specific timescales, consistently with intrinsic neural firing patterns (Gao et al. 2020) and underlying mental processes (Van De Ville et al. 2021). This raises the question of how functional acquisition timescales may affect subject identification within this functional fingerprinting framework.

Understanding the effect of temporal resolution (TR) on fingerprinting of resting-state fMRI (rs-fMRI) holds relevance for several reasons. First, rs-fMRI has gained widespread use in both basic and clinical research, making it crucial to comprehend the factors influencing its outcomes (Lee, Smyser, and Shimony 2013a; Smitha et al. 2017). Second, the growing influence of the open-science policy has encouraged access to multicentric rs-fMRI datasets acquired using different TRs, emphasizing the need to examine the implications of this factor on data interpretation and integration (e.g., https://openfmri.org, https://adni.loni.usc.edu, http://www.humanconnectomeproject.org, http://www.developingconnectome.org, https://www.ukbiobank.ac.uk, https://fcon_1000.projects.nitrc.org/indi/CoRR/html/ among various other public rs-fMRI data sources). Lastly, advancements in rapid parallel imaging technologies (Larkman et al. 2001) have enabled neuroscientists to obtain whole-brain images with sub-second sampling rates, thus allowing the investigation of neural dynamics with greater precision and flexibility (Akin et al. 2017; Lee et al. 2013b; Zalesky et al. 2014). However, the reliability of fast fMRI remains unclear. On the one hand, acquiring a higher number of timepoints without increasing the scanning duration enhances statistical power (Dowdle et al. 2021; Feinberg et al. 2010; Posse et al. 2012; Smith et al. 2013). On the other hand, speed comes at the cost of lower signal-to-noise ratio per time frame (Barth et al. 2016; Boubela et al. 2014; Edelstein et al. 1986; Feinberg and Setsompop 2013; Preibisch et al. 2015) with respect to conventional fMRI protocols (TR ~2–3 s), with the ultimate result of decreasing the statistical validity of inferences about intrinsic FC (Corbin et al. 2018). To the best of our knowledge, very few studies have assessed test–retest reliability in fast fMRI (Jahanian et al. 2019) or in comparisons between different TRs. In the few instances where such comparisons were made, data were downsampled (Birn et al. 2013; Huotari et al. 2019; Shah et al. 2016) rather than acquired in distinct fMRI runs with different TRs, which is not equivalent. Consequently, the impact of acquisition's TR on rs-fMRI fingerprinting remains largely unexplored.

The relevance of this research question lies not only in the potential implications for the reproducibility and generalizability of fMRI results, but it is also linked to the open field of investigation of the temporal aspects of brain fingerprints. In general, fast fMRI has been proven to better capture complex temporal features of the fMRI signal which carry meaningful information about brain states (Dowdle et al. 2021; Yang and Lewis 2021). Interestingly, in the specific framework of connectome fingerprinting, fast fMRI has provided insights into which specific time scales of connectivity patterns are more highly related to the individuality of cognitive functions (Van De Ville et al. 2021). Evaluating how brain fingerprints are affected by TR may shed light on what exactly is the information encoded in brain connectomes that ultimately makes us unique, and, specifically, weather this information unfolds in possibly preferential windows in time, when one individual's brain is maximally identifiable (Van De Ville et al. 2021). In this scenario, exploring which TR can optimize the investigation of brain fingerprints' time scales, in a network- and region-specific fashion,

could advance our knowledge on mental process and cognition, with potential applications in the emerging fields of precision medicine.

In this study, we extend the investigation of temporal features of spontaneous brain fMRI fingerprints by addressing the question of whether the TR of rs-fMRI acquisitions' influences healthy subject identification. We thus present the application of the "identifiability framework" (Amico and Goñi 2018) to a nowadays still unexplored scenario. Specifically, for each subject ($N = 20$), we collected rs-fMRI data with five different TRs, ranging from 0.5 to 3 s. Our analyses focused on evaluating the test–retest reliability at the whole-brain level by considering the following aspects: (i) the impact of TR on subject identifiability when comparing data acquired with the same TR; (ii) the influence of TR on subject identifiability when comparing data acquired with different TRs; (iii) the effect of the number of acquired timepoints (i.e., volumes) on test–retest reliability; (iv) the differential contribution of specific brain regions and functional networks to subject identifiability, regardless of TR, and to TR identifiability across subjects.

2 | Materials and Methods

A subset of the data used in the current study was also employed in a previous work (Saviola et al. 2022), available on bioRxiv. Therefore, participants' demographics, data acquisition, and pre-processing steps were already partially described there but are reiterated here for the sake of completeness and with the necessary modifications.

2.1 | Participants

A total of 20 healthy volunteers (10 females, age: 24 ± 3 years, 4 left-handers) without neurological and/or psychiatric disease history gave written informed consent to participate in this study, which was approved by the Ethical Committee of the University of Trento, Italy.

2.2 | MRI Acquisition

Neuroimaging data were acquired with a 3 Tesla Siemens Magnetom Prisma (Siemens Healthcare, Erlangen, Germany) whole body MRI scanner equipped with a 64-channel receive-only head–neck RF coil. Each participant underwent one structural T1-weighted standard MPRAGE (TR/TE = 2.31 s/3.48 ms, 1 mm isotropic voxels), and five runs of resting-state functional MRI (rs-fMRI, TE = 28 ms, 3 mm isotropic voxels, FA = 59°, simultaneous multi slice acceleration factor = 6, 56 slices, fat suppression, interleaved slice acquisition, 0 mm slice gap, anterior-to-posterior phase-encoding) during the same day. Acquisition parameters for the five rs-fMRI runs were identical except for TR, which was manipulated such that the total scanning time was kept constant (7.4 min), thus affecting the total number of brain functional volumes (NoV acquired) per run: TR(s)/NoV = 0.5/905; 0.7/646; 1/452; 2/226; 3/150. Nine participants underwent the five acquisition runs from the shortest to the longest TR, while the remaining 11 participants underwent the acquisitions from the longest to the shortest TR. The order of the five TR runs was not fully randomized across participants in order to avoid potential biases due to the coil heating and amount of movement, which are higher for shorter than for longer TRs. Finally, a phase and magnitude double-echo gradient echo structural sequence was used to derive a magnetic field map for geometric distortion correction (TR = 682 ms, $TE_1 = 4.2$ ms, $TE_2 = 7.4$ ms, 3 mm isotropic voxels).

2.3 | Data Preprocessing and Functional Connectivity Matrices

Brain rs-fMRI data were preprocessed using FSL (Jenkinson et al. 2012) and following standard steps: (i) slice timing and head motion correction (see Section S5 for DVARS); (ii) T1-weighted image tissue segmentation; (iii) co-registration of the rs-fMRI time-series to the T1-weighted image; (iv) rs-fMRI temporal band-pass filtering; (v) nuisance regression of the six head motion, white matter, and cerebrospinal fluid signals; (vi) normalization to standard MNI template space; (vii) spatial smoothing with a 6 mm FWHM kernel size. Instead of applying one of the traditional temporal band-pass filters (i.e., [0.01–0.08] Hz or [0.01–0.1] Hz), we opted for a [0.01–0.3] Hz filter which could allowed us to censor physiological noise at the fastest TRs, where the denoising procedure is more effective (Jahanian et al. 2019). We then applied the same filter to the other TRs in order to avoid introducing a variability factor which would potentially bias the main analysis. Specifically, the band-pass filter we applied allowed us to avoid the frequency bands (i.e., ∼0.9 Hz at TR 0.5 s, and ∼0.3 Hz at TR 0.7 s) at which the cardiac noise aliases at our fastest TRs, without removing relevant neural frequencies.

After pre-processing, rs-fMRI images were parcellated using the Glasser multimodal parcellation atlas (Glasser et al. 2016), consisting of 360 cortical parcels. For full gray matter coverage (Amico and Goñi 2018), we added 19 parcels from a subcortical atlas provided by the Human Connectome Project (HCP; Van Essen et al. 2013, release Q3, filename "Atlas_ROI2.nii.gz"). Since the choice and resolution of the parcellation atlas can affect between-subject and within-session differences in FC estimation (Ahrends et al. 2022; Pervaiz et al. 2020), we reran all analysis using the functional atlas of Schaefer et al. (2018) with 100 parcels, instead of the Glasser atlas.

FC matrices were calculated for each subject and TR by estimating the Pearson's correlation coefficients between all parcels' rs-fMRI time courses. The FC matrices were symmetric and were kept neither thresholded nor binarized in the following analysis (Amico and Goñi 2018).

2.4 | Group-Level PCA

In order to investigate the effect of TR on individual FC identifiability, we performed two types of fingerprinting analysis (Figure 1): (i) a within-TR analysis considering, for every subject and every TR separately, FC matrices computed on the first half of the rs-fMRI time course (half volumes) as test, and FC matrices computed on the second half of the rs-fMRI time course as retest (Amico and Goñi 2018); (ii) a between-TR analysis

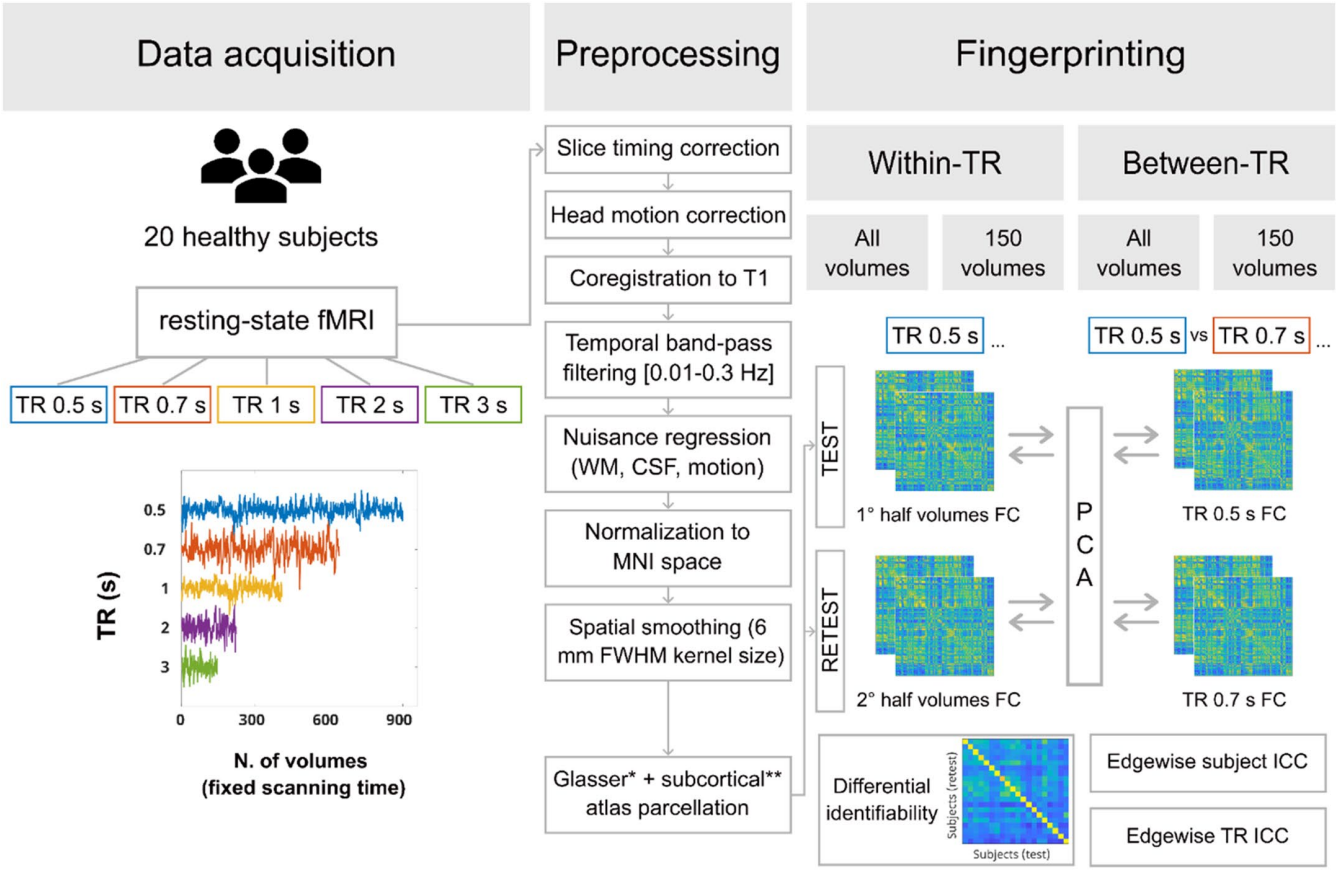

FIGURE 1 | Analysis workflow. Resting-state fMRI data were acquired for each subject during five runs differing in TR (TR = 0.5 s, 905 volumes; TR = 0.7 s, 646 volumes; TR = 1 s, 452 volumes; TR = 2 s, 226 volumes; TR = 3 s, 150 volumes). After preprocessing, parcellation was performed on the basis of an atlas combining Glasser parcellation (Glasser et al. 2016) and a subcortical parcellation provided by the Human Connectome Project. Two fingerprinting analyses were performed. Within-TR analysis: After parcellation, for each TR separately, time course was split in two halves, and two sets of functional connectivity (FC) matrices (test and retest) were computed as input for the group-level principal component analysis (PCA). FC matrices were then reconstructed using the optimal number of PCA components. Between-TR analysis: After parcellation, for each TR pairwise comparison, the whole time course from two different TR runs (test and retest) was used to compute FC matrices. The optimal number of components resulting from the group-level PCA were used to reconstruct back each FC matrix. For both the within-TR and the between-TR analysis, Pearson's correlation coefficients were computed between test and retest sets of FC matrices, in order to create an identifiability matrix for each TR condition and TR pairwise comparison. Finally, edgewise intraclass correlation (ICC) was computed in two different ways, resulting in a subject and a TR ICC. The whole fingerprinting analysis was repeated using all volumes and only the first 150 volumes of each TR run. CSF, cerebrospinal fluid; FC, functional connectivity; ICC, intraclass correlation; PCA, principal component analysis; WM, white matter. *Glasser et al. (2016); **Human Connectome Project, release Q3.

considering, for every subject and all TR pairwise comparisons (i.e., TR 0.5 vs. TR 0.7, TR 0.5 vs. TR 1, etc.), FC matrices computed on one TR data as test, and FC matrices computed on the other TR data as retest. Note that since labeling a set of FC matrices as test or retest in a specific comparison did not elicited differences in analysis and results, we here report findings only from one possible test–retest combination (e.g., only TR 0.5 vs. TR 0.7 s results are reported because they are identical to TR 0.7 vs. TR 0.5 s results).

Since the rs-fMRI runs were identical in the total scanning time but they differed in TR, FC matrices were estimated on a different number of brain volumes, which could affect subject identifiability (Anderson et al. 2011; Birn et al. 2013; Noble et al. 2017, Van De Ville et al. 2021). To evaluate this, we repeated both the within-TR and the between-TR analysis using only the first 150 volumes (i.e., the number of volumes of the slowest TR) of each TR time course. This disentangled the effect of number of volumes from the effect of TR on individual FC identifiability.

For both the within- and between-TR analysis, when using both all volumes and only the first 150 volumes, we applied the denoising procedure for maximizing connectivity fingerprints in human connectomes first introduced by Amico and Goñi (2018). This procedure was based on a PCA (Jolliffe 2014) for extracting the optimal number of connectivity-based components that maximizes subject identifiability. The rationale behind this analysis is that high-variance components may carry cohort-level FC information, lower-variance components may carry individual-level FC information, and the lowest-variance components may carry noisy or artefactual FC information (Amico and Goñi 2018). By iteratively exploring the number of components used, individual-level components can be identified in a data-driven way while artefactual-level components can be

discarded. Briefly, for each subject, two FC matrices (test and retest as described in the previous paragraphs) were taken as input, their upper triangle was vectorized, and then added to a matrix having one test and one retest column for each subject, and FC edge weights as rows. Once extracted the main connectivity-based principal components (PCs), each individual FC matrix is reconstructed back based on its mean and the linear combination of the chosen PCs.

Except for data preprocessing, analysis was conducted using MATLAB (2017b). The code for performing the fingerprinting analysis was adapted from the scripts publicly available at Enrico Amico's GitHub repository (https://github.com/eamico).

2.5 | Whole-Brain Connectome Fingerprinting: Differential Identifiability and Success Rate

In order to assess the identifiability of FC profiles of single individuals among the entire sample at the whole-brain level, an identifiability matrix (Amico and Goñi 2018) was created where rows referred to subjects' test FCs, columns to retest subjects' FCs, and the Pearson's correlation coefficient was used to compute their similarity. The average of the main diagonal elements of the identifiability matrix (multiplied by 100) is defined as "self-identifiability" or "*Iself*" since it is a measure of the similarity of the same subject's FC profile between test–retest data. The average of the main off-diagonal elements of the identifiability matrix (multiplied by 100), instead, is defined as "*Iothers*" and represents the similarity of FC profiles between test–retest data across subjects. The assumption of the functional connectome fingerprint is that FC should be, overall, more similar between test–retest data of the same subject than between different subjects. Thus, a "differential identifiability" or "*Idiff*" measure ($Idiff = Iself - Iothers$) has been proposed as a group estimate of how much an individual FC profile is identifiable amongst the whole sample (Amico and Goñi 2018). With this formalism, *Idiff* represents a continuous score for the level of individual whole-brain fingerprinting present on a set of test–retest functional connectomes. We also computed a binary identification score, namely "success rate" (*SR*), which is defined as the percentage of subjects whose identity was correctly predicted out of the total number of subjects (Finn et al. 2015). Consistent findings between *Idiff* and *SR* would suggest the possibility to generalize our subject identification results to different identifiability scores (Sareen et al. 2021).

2.6 | Local Contributions to Fingerprinting: The Role of Individual Edges and Networks

The fingerprinting analysis described in the previous paragraphs aimed at evaluating whether the whole brain FC could successfully lead to a subject identification between test and retest datasets acquired with the same or with different TRs. However, it does not mean that the same specific connectome edges (functional correlations between brain parcellation pairs) were equally responsible for identifiability in all the different test–retest comparisons. In fact, this does not even mean that the most stable edges between test–retest comparisons were the same edges that contributed most to successful subject identifiability (Dufford et al. 2021). In order to investigate which specific edges and networks (grouping edges) were the most reliable in identifying subjects across TRs (regardless of specific test–retest comparisons), we computed the intraclass correlation coefficient (ICC; Bartko 1966; McGraw and Wong, 1996), as in previous studies (Amico and Goñi 2018; Bari et al. 2019; Noble et al. 2017; Sareen et al. 2021; Van De Ville et al. 2021; Wang et al. 2021).

ICC is a statistical measure of the agreement between units of (or ratings/scores) of different groups (or raters/judges). The stronger the agreement, the higher its ICC value. ICC can be interpreted as <0.4 = poor; 0.4–0.59 = fair; 0.60–0.74 = good; and >0.74 = excellent (Cicchetti and Sparrow 1981). We employed ICC to quantify the extent to which individual edges can separate between subjects (raters) by remaining reliable within subjects across the different TRs (units). Specifically, for each edge we computed the ICC(1,1) variant (Bari et al. 2019). The higher the ICC, the higher the edge contribution to subject identifiability regardless of the TR. From now on, we will refer to this measure as "subject ICC." Given the small sample size, a bootstrap procedure was applied when computing ICC, as suggested by Bari et al. (2019): over 100 iterations, 75% of the subjects were randomly selected, and the ICC was calculated for each edge and stored in a square symmetric matrix having edges of size N^2, where N is the number of edges. The resulting ICC matrices over all iterations were then averaged to obtain the final subject ICC values.

We then computed ICC considering TRs as raters and subjects as units. In this "TR ICC," the higher an edge ICC, the higher the edge contribution to distinguish between TRs regardless of subjects.

2.7 | Statistical Analysis

A permutation testing framework (Sareen et al. 2021) was employed to assess the statistical significance of the observed *Idiff* and *SR* values computed from the identifiability matrices: over 1000 iterations, subjects' test–retest FC matrices were randomly shuffled, and the *Idiff* and *SR* were computed on the resulting randomized identifiability matrices, in order to create two non-parametric null distributions, respectively for *Idiff* and *SR*. Moreover, to correct for multiple comparisons, we merged the null distributions from all the five TRs in the within-TR analysis, and from all the TR pairwise comparisons in the between-TR analysis. The observed *Idiff* and *SR* values were then compared against their corresponding null distribution, such that the computed *p*-values are the proportion of values in the null distribution greater or equal to the observed values (Nichols and Holmes 2002).

Furthermore, distributions of *Idiff*, *Iself*, *Iothers*, and *SR* on a subject level (Bari et al. 2019) were calculated in order to: (i) compare differential identifiability (*Idiff*) computed on the original FC matrices (before PCA) to the *Idiff* computed on the PCA-reconstructed FC matrices (both within-TR and between-TR identifiability); (ii) compare FC identifiability in one TR against FC identifiability in all the other TRs (within-TR analysis); (iii) compare FC identifiability in one TR comparison against FC

identifiability in all the other TR pairwise comparisons (between-TR analysis); (iv) compare FC identifiability computed on all volumes against FC identifiability computed only on the first 150 volumes (both within-TR and between-TR identifiability). In particular, the distributions of the subject-level values of *Iself* (main diagonal elements of the identifiability matrix), *Iothers* (average of the off-diagonal elements of the identifiability matrix computed for each subject) and *Idiff* (difference between subject-level *Iself* and subject-level *Iothers* values) were compared using a two-tailed Wilcoxon signed rank test, followed by a false discovery rate (FDR) correction applied within each metric test. Statistical differences in *SR*, instead, were assessed by assigning a binary score to each subject (1 if the subject-level *Iself* value was higher than the subject-level *Iothers* value, meaning that the subject was correctly identified among the sample; 0 otherwise) and using the exact version of a two-tailed McNemar's test for proportions in paired samples, followed by an FDR correction.

Significance threshold after FDR correction was declared at α level = 0.05. Statistical analysis was performed using R Studio (R Core Team 2013).

3 | Results

3.1 | Whole-Brain Within-TR Connectome Fingerprinting: The Effect of Acquisition TR and Number of Volumes

We first investigated how the TR at which rs-fMRI data were acquired affected the possibility to identify one individual among the whole sample only on the basis of whole-brain resting-state FC profiles (within-TR fingerprinting).

As a result of the group-level PCA, FC matrices for each subject and each TR were reconstructed using a number of PCs equal to the sample size (optimal number of PCs maximizing *Idiff*: $m^* = 20$; Table 1; see also Section S1 and Figure S1A). We found that the *SR* at which subjects were identified based on their FC was equal to 100% within all TR runs except two (TR 0.7 s: *SR* = 97.5%; TR 2 s: *SR* = 95%). When comparing observed *SR* and *Idiff* computed on the single identifiability matrices against their correspondent null distributions (Sareen et al. 2021; see Section 2), a statistically significant effect was obtained (permutation testing, $p < 0.001$) for each TR. Taken together, these results suggested that, independently of TR, PCA-based reconstruction of FC ensured a successful subject identifiability (Figure 2A).

However, pairwise within-TR *Idiff* comparisons (Figure 2B) revealed that *Idiff* at TR 0.5 s was significantly higher than *Idiff* from all other TRs ($p_{FDR} < 0.05$, Wilcoxon test, Table 2), and that TR 3 s significantly outperformed TR 0.7, 1, and 2 s in *Idiff* ($p_{FDR} < 0.05$, Wilcoxon test, Table 2. See also Section S4 for effect sizes). To better explore what drove this U-shaped effect of TR in *Idiff* (Figure 2B), we looked at the trajectories of *Iself* and *Iothers* distributions separately. We found (Table 2) that at TR 0.5 s, *Iself* resulted to be significantly higher than at all other TRs. Instead, *Iothers* were significantly lower at TRs 0.5 and 3 s, thus giving the inverse U-shaped trend with respect to *Idiff*. The comparisons of *SR* distributions between TRs, instead, did not reveal any significant effect.

Similar results were found when using only the first 150 volumes instead of the whole rs-fMRI time course for the fingerprinting analysis (Section S2, and Tables S3 and S4). No significant differences were observed in any TR condition when comparing *Idiff* and *SR* in the 150 volumes with their corresponding distributions in the analysis encompassing the whole time series (Table 2). *Iself* and *Iothers* values, instead, significantly decreased in all TRs (Wilcoxon test, $p_{FDR} < 0.001$, Table 2) when a lower number of volumes was used to estimate subject identifiability.

To summarize the whole-brain within-TR rs-fMRI fingerprinting findings: (i) although subject identifiability is consistently high across the TRs evaluated, it is significantly maximized at TR 0.5 and 3 s, a pattern that appears driven by lower across-subjects variability at those TRs; (ii) the number of rs-fMRI volumes does not significantly affect identifiability, regardless of TR. These results were also replicated using the non-PCA-reconstructed FC matrices (Section S1) as well as a different parcellation resolution (Section S7).

3.2 | Whole-Brain Between-TR Connectome Fingerprinting: The Effect of Acquisition TR and Number of Volumes

Next, we proceeded to investigate the impact of TR on subject identifiability across different TR runs. FC matrices for each TR pairwise comparison were reconstructed using a number of PCs close to the sample size ($m^* = 20.7 \pm 0.68$, Table 3; Section S1

TABLE 1 | Within-TR analysis summary table.

TR (s)	m^*	R^2	$Idiff_{orig}$	$Idiff_{recon}$	$Iself_{recon}$	$Iothers_{recon}$	SR_{orig}	SR_{recon}
0.5	20	0.84	38.52	64.19	96.34	32.15	100.00	100.00
0.7	20	0.85	27.32	46.45	91.15	44.71	97.50	97.50
1	20	0.86	25.57	44.07	92.83	48.76	97.50	100.00
2	20	0.87	25.20	43.77	91.44	47.67	95.00	95.00
3	20	0.84	32.03	56.23	93.36	37.13	100.00	100.00

Note: For each TR, values of the percentage differential identifiability (*Idiff*), self-identifiability (*Iself*), others-identifiability (*Iothers*), and success rate (*SR*) are reported for the all volumes condition. Orig values were computed on the identifiability matrices derived from the original (before principal component analysis reconstruction) functional connectivity matrices, while Recon values were extracted from the FC matrices reconstructed by using the optimal number of principal components (m^*), for which explained variance (R^2) is also reported.

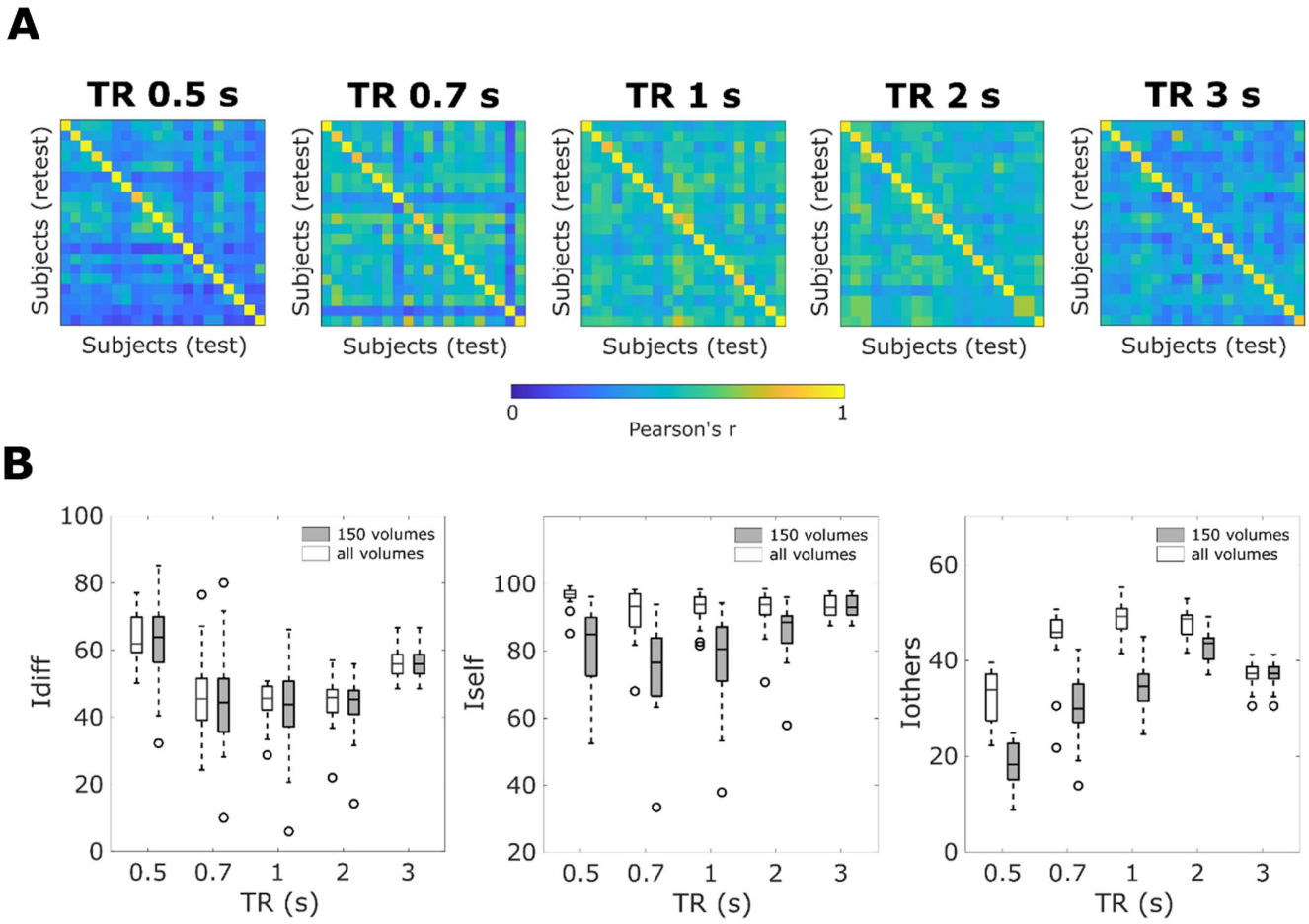

FIGURE 2 | Within-TR fingerprinting. (A) Identifiability matrices of PCA-reconstructed functional connectivity profiles, extracted from the whole scanning time course, separately for each TR run. (B) Box plots of differential identifiability (*Idiff*), self-identifiability (*Iself*), and others-identifiability (*Iothers*) distributions computed at a subject-level after PCA-reconstruction, when using all (white) and 150 (gray) volumes for the fingerprinting analysis.

and Figure S1C). The comparison between observed *SR* and *Idiff* against their corresponding null distributions (Sareen et al. 2021; see Section 2) resulted in a statistically significant effect (permutation testing, $p < 0.001$). As a consequence, even if identifiability metrics showed lower values than in the within-TR analysis, PCA-based reconstruction of FC still proved to allow a successful subject identifiability.

Additionally, we explored differences in identifiability metrics between TR pairwise combinations. Despite not always surviving FDR correction, we found a non-significant trend ($p_{FDR} > 0.28$) according to which higher similarity between TRs resulted in higher identifiability as measured by *Idiff and SR* (Figure 3 and Table 4; see also Section S4 for effect sizes). Moreover, *Idiff* and *SR* between close but slow TRs (i.e., 2 and 3 s) tended to be higher than between close but fast TRs (i.e., 0.5 and 0.7 s), despite the absolute difference in TR being higher in the former (1 s) rather than in the latter case (0.2 s) (Figure 3B,C). The same trend was observed when considering the separate contributions of *Iself* and *Iothers* to subject identifiability (Figure S5), with *p* values surviving FDR correction in several TR combinations (Table S5).

When using only the first 150 volumes, instead of the whole time course for the fingerprinting analysis, PCA-based reconstruction of FC still proved to allow a successful subject identifiability for all pairwise TR combinations (Section S3). However, relative to the use of the full time series, using only the first 150 rs-fMRI volumes had some identifiability costs: the variability of *ldiff* was higher (Table 3), and *SR* was on average lower ($68.5\% \pm 20.35$) with respect to the full time course ($82.5\% \pm 11.49$). Notably, when comparing the *Idiff* and *SR* of each TR pairwise combination in the 150 volumes with their corresponding values in the all volumes analysis, we found that, when using less timepoints, *Idiff* was significantly lower in most TR combinations involving fast TRs (i.e., TR 0.5 and TR 0.7 s), while no *SR* value comparison survive FDR correction (Table 4). A significant decrease of *lself* and *lothers* was observed in the 150 volumes condition (Table S5) for most TR combinations.

To summarize the whole-brain across-TR fingerprinting findings: (i) subject identifiability tends to be higher for rs-fMRI acquisition protocols using similar TRs; (ii) using the first 150 rs-fMRI volumes decreases identifiability performance with respect to the use of the full acquired time series for each TR. These results were also replicated using the non-PCA-reconstructed FC matrices (Section S1) as well as a different parcellation resolution (Section S7).

3.3 | Local Contributions to rs-fMRI Fingerprinting: Identifiability of Subjects Across TRs and Identifiability of TRs Across Subjects

The within- and between-TR analysis discussed in the previous paragraphs referred to the whole brain FC profiles. To explore whether specific edges or brain regions contributed more than others to subject identifiability over all TRs, we computed a subject ICC. Edges showed a subject ICC ranging from poor (−0.063) to fair (0.429), with a mean of -0.0028 ± 0.04. By averaging ICC values according to Yeo functional networks, we found that within- and between-network connections involving high-level associative areas—that is, brain regions belonging to default mode network and ventral attention network (Damoiseaux et al. 2006)—had a more prominent role in separating between subjects, regardless of TR (Figure 4A,C,E).

Edgewise TR ICC values ranged from poor (−0.013) to excellent (0.764), with a mean of 0.329 ± 0.114. As an opposite pattern with respect to subject ICC, low-level areas—comprising visual and subcortical regions (Damoiseaux et al. 2006; Xu, Hanganu-Opatz, and Bieler 2020)—appeared among the top 5 networks implicated in distinguishing between TRs, regardless of subjects (Figure 4B,D,F). TR ICC values were overall significantly lower with respect to subject ICC values (Wilcoxon rank sum test: $p < 0.001$), suggesting that variability in edgewise FC was more affected by differences in acquisition protocols than by between-subjects differences.

Finally, it is interesting to note that both subject and TR ICC results did not qualitatively change much when rerunning the analysis taking into account only the first 150 volumes of each run (Figure S7).

4 | Discussion

In this study, we employed brain connectome fingerprinting enriched by group-level PCA to assess subject identifiability across rs-fMRI protocols with varying TR. We replicated the finding that intrinsic FC is unique and sufficient to identify an individual among a sample of healthy subjects (Amico and Goñi 2018;

TABLE 2 | Within-TR statistics summary table.

			p_{FDR} (Wilcoxon)			
		TR (s)	**0.5**	**0.7**	**1**	**2**
All volumes	Idiff	**0.7**	$\mathbf{1.26 \times 10^{-4}}$**	—	—	—
	Iself		**0.02***	—	—	—
	Iothers		$\mathbf{1.91 \times 10^{-5}}$**	—	—	—
	SR		1.00	—	—	—
	Idiff	**1**	$\mathbf{4.77 \times 10^{-6}}$**	0.43	—	—
	Iself		**0.04***	0.99	—	—
	Iothers		$\mathbf{4.77 \times 10^{-6}}$**	$\mathbf{5.37 \times 10^{-4}}$**	—	—
	SR		1.00	1.00	—	—
	Idiff	**2**	$\mathbf{4.77 \times 10^{-6}}$**	0.99	0.43	—
	Iself		**0.02***	0.99	0.99	—
	Iothers		$\mathbf{4.77 \times 10^{-6}}$**	0.17	0.14	—
	SR		1.00	1.00	1.00	—
	Idiff	**3**	$\mathbf{5.37 \times 10^{-4}}$**	$\mathbf{4.50 \times 10^{-3}}$*	$\mathbf{4.77 \times 10^{-6}}$**	$\mathbf{4.77 \times 10^{-6}}$**
	Iself		**0.01***	0.99	0.99	0.99
	Iothers		$\mathbf{1.79 \times 10^{-3}}$*	$\mathbf{1.21 \times 10^{-3}}$*	$\mathbf{4.77 \times 10^{-6}}$**	$\mathbf{4.77 \times 10^{-6}}$**
	SR		1.00	1.00	1.00	1.00
All vs. 150 volumes	*Idiff*		0.76	0.76	0.76	0.76
	Iself		$\mathbf{2.29 \times 10^{-5}}$**	$\mathbf{1.09 \times 10^{-4}}$**	$\mathbf{9.54 \times 10^{-5}}$**	$\mathbf{7.23 \times 10^{-4}}$**
	Iothers		$\mathbf{2.54 \times 10^{-6}}$**	$\mathbf{2.54 \times 10^{-6}}$**	$\mathbf{2.54 \times 10^{-6}}$**	$\mathbf{9.56 \times 10^{-5}}$**
	SR		1.00	1.00	1.00	1.00

Note: For each TR comparison, *pFDR* values are reported for the all volumes analysis (*$p_{FDR} < 0.05$, **$p_{FDR} < 0.001$). Moreover, for each TR, *pFDR* values resulting from the comparison between the all volumes and the 150 volumes distributions are summarized. Wilcoxon signed rank was used for differential identifiability (*Idiff*), self-identifiability (*Iself*) and others-identifiability (*Iothers*), while McNemar's test for proportions in paired samples was employed for success rate (*SR*). Statistics refer to functional connectivity matrices reconstructed by using the optimal number of principal components.

TABLE 3 | Between-TR analysis summary table.

TR (s)	m^*	R^2	$Idiff_{orig}$	$Idiff_{recon}$	$Iself_{recon}$	$Iothers_{recon}$	SR_{orig}	SR_{recon}
[0.5, 0.7]	21	0.85	17.95	30.25	75.39	45.14	70.00	67.50
[0.5, 1]	20	0.84	16.19	28.70	76.24	47.54	70.00	77.50
[0.5, 2]	20	0.84	13.32	25.87	73.47	47.61	67.50	72.50
[0.5, 3]	20	0.81	12.93	26.37	69.56	43.19	50.00	62.50
[0.7, 1]	21	0.89	23.02	35.26	88.26	53.00	87.50	92.50
[0.7, 2]	21	0.89	19.63	32.22	85.11	52.89	85.00	90.00
[0.7, 3]	22	0.87	17.98	31.73	77.35	45.63	72.50	87.50
[1, 2]	20	0.89	22.73	36.23	92.29	56.05	92.50	92.50
[1, 3]	21	0.86	19.39	35.24	84.47	49.24	82.50	92.50
[2, 3]	21	0.87	20.61	35.78	85.20	49.42	85.00	90.00

Note: For each TR combination, values of the percentage differential identifiability (*Idiff*), self-identifiability (*Iself*), others-identifiability (*Iothers*), and success rate (*SR*) are reported for the all volumes condition. Orig values were computed on the identifiability matrices derived from the original (before principal component analysis reconstruction) functional connectivity matrices, while Recon values were extracted from the FC matrices reconstructed by using the optimal number of principal components (m^*), for which explained variance (R^2) is also reported.

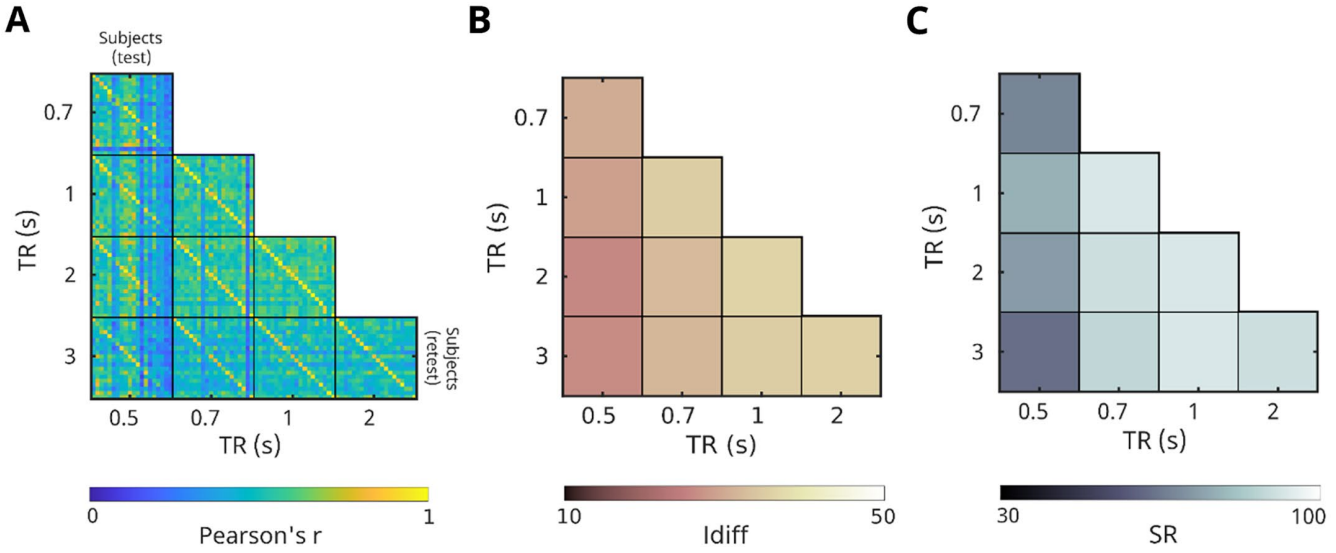

FIGURE 3 | Between-TR fingerprinting. (A) Identifiability matrices of the PCA-reconstructed functional connectivity profiles, extracted from the whole scanning time course, separately for each TR combination. (B) Confusion matrices of the differential identifiability (*Idiff*) values computed from the between-TR identifiability matrices (A). (C) Confusion matrices of the success rate (*SR*) values computed from the between-TR identifiability matrices (A).

Bari et al. 2019; Finn et al. 2015; Romano et al. 2022; Sareen et al. 2021; Sorrentino et al. 2021; Svaldi et al. 2021; Troisi Lopez et al. 2023; Van De Ville et al. 2021). We further extended these results by proving that, despite the high identifiability achieved regardless of the TR at which data were acquired, fingerprinting analysis was still sensitive to the fMRI acquisition protocol, and in particular to TR. This allowed us to dig into the still unresolved question of test–retest reliability in fast fMRI approaches (Jahanian et al. 2019; Polimeni and Lewis 2021), and to make specific considerations about pooling data acquired with different BOLD signal sampling rates, which has useful applications in neuroscientific research, in both clinical and computational neuroimaging. In particular, based on our evidence on functional fingerprinting, we recommend (i) pooling data acquired using the same TR rather than different TRs; (ii) if condition (i) can be met, preferably acquire data using very fast (TR 0.5 s) or very slow (TR 3 s), although intermediate TRs also guarantee a successful subject identifiability; (iii) if condition (i) cannot be met, pooling data with close TRs and better if they are slow; (iv) increasing scanning length only if data are acquired using different TRs; (v) mainly relying on higher-level cognitive brain areas for subject identifiability.

4.1 | Within-TR Subject Identifiability Is Maximized at TR 0.5 and 3 s

Although in the within-TR analysis subject identifiability was successful regardless of TR, we showed that *Idiff* was maximized at TR 0.5 and 3 s, while significantly decreasing at TR 0.7, 1, and

2 s. These findings can be explained by considering that test–retest reliability of resting state fMRI data is largely affected by the noise introduced by scanner artifacts, subject movements, changes in cognitive or emotional states, and, importantly, by physiological factors (Caballero-Gaudes and Reynolds 2017). Cardiorespiratory brain pulsations are temporally correlated with the BOLD fMRI signal, which means that in typical rs-fMRI protocols with TRs ~2 s, these confounding components are added up to and can mask the intrinsic neural signal (Özbay et al. 2019). In fact, FC BOLD fluctuations predominantly lie below 0.1 Hz frequencies (Cordes et al. 2001), thus a low-pass filter is commonly applied to retain only frequencies below this threshold, and to remove signal from non-neuronal sources, such as respiratory rate (0.2–0.3 Hz; Kiviniemi et al. 2016) and cardiac pulsations (0.8–1.2 Hz; Kiviniemi et al. 2016). However, this denoising procedure is effective only when TR is short (< 0.5 s; Jahanian et al. 2019; Liu 2016; Reynaud et al. 2017), reducing the noise components in the signal and thus improving test–retest reliability (Jahanian et al. 2019). Instead, when TR is higher than 0.5 s, cardiac fluctuations are undersampled and aliased into the lower frequency range, which makes physiological noise difficult to remove with band-pass filtration (Lowe, Mock, and Sorenson 1998; Huotari et al. 2019). The consequent increase of aliased noise in the signal is consistent with the significantly lower differential identifiability we registered in TR 0.7, 1, and 2 s runs. As further evidence, not applying any band-pass filter significantly decreased identifiability at TR 0.5 s, while it increased at TRs higher than 0.5 s (see Section S6). Finally, at TR 3 s, according to the Nyquist theorem, the BOLD signal is sampled at ~0.16 Hz, implicitly low-pass filtering respiratory and cardiovascular noise (Huotari et al. 2019), which is consistent with the improved test–retest reliability. A simulation is included in the Supporting Information Appendix to further support this explanation.

4.2 | Between-TR Subject Identifiability Is Maximized When TRs Are More Similar

Subject identifiability was successful even when considering rs-fMRI acquisitions with different TRs. However, identifiability gradually decreased as TRs became more dissimilar. This

TABLE 4 | Between-TR statistics summary table.

			p_{FDR} (Wilcoxon)									
		[TR*i*, TR*j*] (s)	**[0.5, 0.7]**	**[0.5, 1]**	**[0.5, 2]**	**[0.5, 3]**	**[0.7, 1]**	**[0.7, 2]**	**[0.7, 3]**	**[1, 2]**	**[1, 3]**	**[2, 3]**
All volumes	Idiff	[0.5, 1]	0.57	—	—	—	—	—	—	—	—	—
	SR		1.00	—	—	—	—	—	—	—	—	—
	Idiff	[0.5, 2]	0.29	0.35	—	—	—	—	—	—	—	—
	SR		0.75	1.00	—	—	—	—	—	—	—	—
	Idiff	[0.5, 3]	0.34	0.78	0.60	—	—	—	—	—	—	—
	SR		1.00	0.91	0.45	—	—	—	—	—	—	—
	Idiff	[0.7, 1]	0.57	0.43	0.28	0.28	—	—	—	—	—	—
	SR		0.07	0.16	0.23	0.07	—	—	—	—	—	—
	Idiff	[0.7, 2]	0.71	0.71	0.34	0.35	0.28	—	—	—	—	—
	SR		0.07	0.16	0.23	0.07	1.00	—	—	—	—	—
	Idiff	[0.7, 3]	0.74	0.71	0.34	0.43	0.57	0.86	—	—	—	—
	SR		0.07	0.16	0.23	0.07	1.00	1.00	—	—	—	—
	Idiff	[1, 2]	0.43	0.57	0.28	0.28	0.90	0.43	0.60	—	—	—
	SR		0.07	0.07	0.09	0.06	1.00	1.00	1.00	—	—	—
	Idiff	[1, 3]	0.60	0.47	0.28	0.28	0.60	0.72	0.85	0.53	—	—
	SR		0.06	0.07	0.07	0.06	0.75	0.75	0.75	1.00	—	—
	Idiff	[2, 3]	0.58	0.53	0.28	0.28	0.73	0.28	0.53	0.70	0.28	—
	SR		0.11	0.16	0.23	0.07	1.00	1.00	1.00	1.00	0.75	—
All vs. 150 volumes	Idiff		0.12	**0.01***	**0.01***	**0.01***	0.06	**0.05***	**0.01***	**0.04***	0.39	0.39
	SR		0.16	0.31	0.16	0.31	0.42	0.56	0.56	0.56	0.42	1.00

Note: For each comparison between TR combinations, p_{FDR} values are reported for the all volumes analysis (*$p_{FDR} < 0.05$, **$p_{FDR} < 0.001$). Moreover, for each TR combination, p_{FDR} values resulting from the comparison between the all volumes and the 150 volumes distributions are summarized. Wilcoxon signed rank was used for differential identifiability (*Idiff*), while McNemar's test for proportions in paired samples was employed for success rate (*SR*). Statistics refer to functional connectivity matrices reconstructed by using the optimal number of principal components.

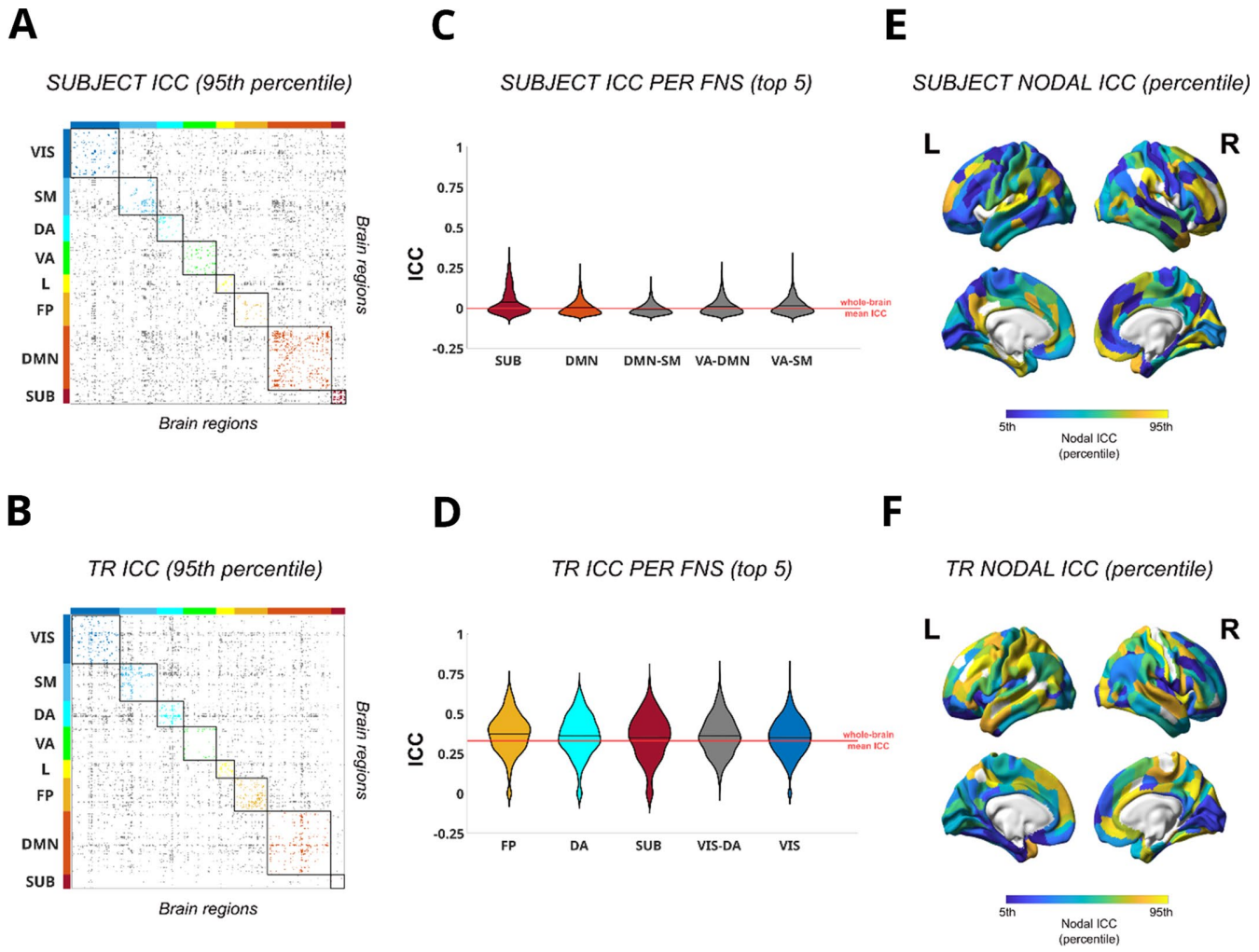

FIGURE 4 | Edgewise intra-class correlation (ICC) analysis of subject identifiability and task identifiability. (A, B) Edgewise subject (A) and TR ICC (B) matrices, showing only functional connections with ICC values significantly higher than the mean distribution (i.e., lying in the 95th percentile). The brain regions are ordered according to Yeo's (Yeo et al. 2011) functional resting state networks (FNs): visual (VIS), somato-motor (SM), dorsal attention (DA), ventral attention (VA), limbic system (L), fronto-parietal (FP), default mode network (DMN), and subcortical regions (SUB). The colored dots refer to within FNs networks edges, while gray dots refer to between FNs networks edges, as in Amico and Goñi (2018). (C, D) Violin plots of edgewise subject (C) and TR (D) ICC distributions for the five FNs with the highest mean ICC value. Each colored violin plot indicates a different within FN, while gray violin plots indicate between FNs ICC distributions. The horizontal solid black line within each violin plot indicates the mean value of each distribution; the solid red line across the violin plots, instead, indicates the whole-brain mean ICC value, as in Amico and Goñi (2018). The most prominent FNs for subject's identifiability (C) resulted: SUB, DMN, and the DMN-SM, VA-DMN, VA-SM interactions. For TR identifiability (D) the most relevant FNs were: FP, DA, SUB, VIS and the VIS-DA interactions. (E, F) Brain renders of nodal ICC, computed as the column-wise mean of the edgewise ICC matrices for both subject (E) and TR (F) ICC, and represented at 5th–95th percentile threshold. Nodal ICC gives an assessment of the overall prominence of each brain region for subject's and TR identifiability. All plots refer to the all volumes analysis. Brain renders were created by running the Matlab code available in the *Surface projection* GitHub repository (https://github.com/rudyvdbrink/Surface_projection, Alexander-Bloch et al. 2018).

confirms the intuition that the more similar the signal sampling, the higher the test–retest reliability. We expanded on this quite trivial finding by showing that identifiability between close but slow TRs (i.e., 2 and 3 s) tended to be higher than identifiability between close but fast TRs (i.e., 0.5 and 0.7 s), despite the absolute difference in TR being higher in the former (1 s) rather than in the latter case (0.2 s). In fact, previous results underlined that physiological (cardiac and respiratory) and low frequency fluctuations reflecting FC exhibited maps increasingly correlated as a function of TR increase, both when considering spatial power and frequency power analysis (Huotari et al. 2019). As a consequence, at close but slow TRs noise is aliased into neural frequency more similarly than in close but fast TRs, which leads to a higher test–retest reliability, even though not significantly different.

4.3 | The Number of rs-fMRI Volumes Affects Between-TR but Not Within-TR Subject Identifiability

Our experimental design used a constant acquisition time for each rs-fMRI run (7.4 min), which led to different number of brain volumes (NoV) for each TR (TR(s)/NoV = 0.5/905;

0.7/646; 1/452; 2/226; 3/150). We investigated the effect of number of volumes on identifiability by using the full time series of each protocol and the first 150 volumes. In both within- and between-TR analysis, subjects could be correctly identified even when a limited number of volumes was used, in agreement with previous literature (Amico and Goñi 2018). However, when comparing data acquired with different TRs, *Idiff* computed on the whole time course was significantly higher than when considering only a subset of volumes. This supports prior evidence that reproducibility improves with longer scanning length, and thus with a larger amount of data (Anderson et al. 2011; Birn et al. 2013; Noble et al. 2017, Van De Ville et al. 2021). When comparing same TR data, instead, the number of volumes did not have any significant impact on *Idiff*. In other words, connectome fingerprinting enriched by group-level PCA was robust enough to guarantee a good test–rest reliability regardless of TR and number of volumes here tested, and, in the most extreme case, even across the equivalent of two acquisitions lasting 1.25 min each at TR 0.5 s (150 volumes). Our findings differ from previous studies suggesting that long scanning acquisitions, ranging from 30 (Gordon et al. 2017; Mueller et al. 2015; Noble et al. 2017) up to 90 min (Laumann et al. 2015), are needed for achieving reliable FC estimates. This disagreement could be due to our use of PCA for group-level fingerprinting denoising and to the fact that our data were collected in a single session. In contrast, previous studies concatenated rs-fMRI data acquired across different days or even months. Indeed, within-session identifiability was found to be significantly higher than between-session identifiability (Dufford et al. 2021).

In addition, our results also challenge the evidence that about 5–10 min of data are sufficient to ensure a stable measurement of connectivity (Choe et al. 2015; Jahanian et al. 2019; Shehzad et al. 2009; Tomasi, Shokri-Kojori, and Volkow 2017; Van Dijk et al. 2010). Instead, our study shows that, even with very short scanning duration, the richness of information coming with higher TR, and thus higher number of acquired timepoints, guaranteed a test–retest reliability as good as when data were acquired with standard protocols (~2–3 TRs). This is consistent with previous findings generated by randomly (Shah et al. 2016) or systematically (Birn et al. 2013; Huotari et al. 2019) downsampling BOLD signal, and by employing feedforward neural networks on an even more limited number of timepoints in fast fMRI acquisitions (TR(s)/NoV = 0.72/100, Sarar, Rao, and Liu 2021).

4.4 | The Contribution of Specific Brain Networks to Edgewise Connectivity to rs-fMRI Fingerprinting

In addition to assessing fingerprinting at whole-brain level, we employed ICC to investigate whether some specific edges will play a differential role in making each individual's functional profile unique. We found that connections within and between DMN and ventral attention network (classically classified as associative areas, Damoiseaux et al. 2006) were the main drivers of subject identifiability. This was in line with prior results (Amico and Goñi 2018; Finn et al. 2015; Van De Ville et al. 2021), but we extended this result by showing that this effect was not impacted by the variability in the TR of the rs-fMRI acquisition protocols.

In order to explain this resting state networks' specific role in subject identifiability, a link can be speculated with the intrinsic neural activity profile and the cognitive processes characterizing these brain circuits (Van De Ville et al. 2021). Previous studies concurred to distinguish between two sets of cortical regions. On one hand, visual, auditory, somatosensory, and motor cortices are mainly responsible for detecting real-time rapid and potentially dangerous changes in the environment. On the other hand, frontal, temporal, and parietal regions, are involved in sustain activity related to working memory (Zylberberg and Strowbridge 2017), decision-making (Gold and Shadlen 2007), hierarchical reasoning (Sarafyazd and Jazayeri 2019), language (Binder et al. 2009), emotion regulation (Laird et al. 2011), and, in general, cognitive processes which require a multimodal integration of information. This differentiation is supported by evidence about synaptic receptor and ion channel gene expression (Cioli et al. 2014), cytoarchitectonic profiles (Gao et al. 2020), gray matter myelination gradients (Huntenburg et al. 2017), functional and anatomical network properties (see Mesmoudi et al. 2013), behavioral gradients (Margulies et al. 2016), and notably, neuronal time scales, with somatomotor regions exhibiting short firing patterns, and associative areas showing longer intrinsic time scales (Gao et al. 2020; Hacker et al. 2017; Runyan et al. 2017).

A relationship between these gradients and human brain identifiability can be hypothesized, by considering that low-level sensory-motor areas are involved in the fast processing of potentially dangerous information coming from the external environment. Thus, they code for a primitive and almost merely evolutionary function, common to all human (and non-human) brains. As such, no fundamental role in distinguishing between single individuals can be attributed to these circuits (Van De Ville et al. 2021). On the contrary, subject connectome uniqueness mainly resides in high-level associative areas, where functional patterns are more decoupled, and thus less predictable on the basis of the structural organization of brain anatomy (Preti and Van De Ville 2019). Moreover, interesting insights might come in the future by investigating the relationship between myelin gradients (higher myelin content in somatomotor that in associative areas, Huntenburg et al. 2017) and brain plasticity (Bonetto et al. 2020): frontal areas are among the last regions to the brain where myelin-associated factors contribute to closing the critical period in the transition between adolescence and adulthood (Crews, He, and Hodge 2007), and play a fundamental role in FC fingerprinting during early brain development (Hu et al. 2022). It is intriguing to think that areas which make us unique are the ones more likely to be affected by experience-based learning and more responsible for reasoning, goal setting, and emotional regulation, but these are only speculations which need fact-based and data-driven investigation (St-Onge et al. 2023).

ICC also allowed us to explore the role of each edge to distinguish between different TR runs. An opposite pattern with respect to edgewise subject identifiability emerged: connections within and between sensory and subcortical areas were shown to contribute to the separation between TRs. These findings can be explained by considering that low-level cognition areas are characterized by a brief transient neural activity which is registered by faster but not by slower TRs. Some contribution to TR identifiability was also shown by high-level circuits, which have longer intrinsic time scales. In other words, information in associative areas

unfolds over a longer period of time, and differences in how often the signal is sampled according to different TRs could affect the amount and type of information registered in these areas at different acquisition TRs. In addition, as discussed in previous paragraphs, aliasing of high frequency noise into lower frequencies spectra is an important factor in separating between TRs, and could specifically interfere with the relevant neural signal from associative areas, characterized by longer time scale activity.

In conclusion, we replicated previous fingerprinting results (Amico and Goñi 2018; Finn et al. 2015; Van De Ville et al. 2021) distinguishing two sets of brain networks which provide different contributions to identifiability. These findings are also consistent with studies investigating the temporal organization of large-scale brain activity, and assigning a key role to dynamic spontaneous transitions between two metastates, a sensorimotor/perceptual and a cognitive/associative one (Vidaurre, Smith, and Woolrich 2017). Our work extends this notion by emphasizing how these metastates affect subject and TR identifiability, and how this identifiability is affected by the fMRI TR.

4.5 | Limitations and Future Directions

This study has a number of limitations. First, the sample size of 20 subjects is limited, despite the fact that each subject underwent five different acquisition runs, thus actually having 100 observations. Second, we did not collect peripheral physiological measures such as cardiac and respiration activity, to verify a uniform physiological state of the subjects across acquisitions with different TRs. Future studies are needed to validate our findings and our explanation of the results, in particular applying band-pass filters (and other denoising pipelines, such as AROMA, FIX, etc.) optimized for the intermediate TRs we here took into account. Moreover, it still remains to be systematically evaluated whether the advantage of applying PCA reconstruction to increase subject identifiability can be generalized, especially to between-group fingerprinting designs with a higher heterogeneity within the cohort's functional connectome profiles (e.g., cross-sectional studies in clinical populations, where the potentially limited shared variance in FC—due to the disease—between patients at different stages and healthy controls, would make it more appropriate to perform PCA on each group separately). As a further matter, we found that brain associative areas gave the highest contribution to fingerprinting regardless of TR. However, Van De Ville et al. (2021) showed that "burst of identifiability" can be detected at fast timescales also in low-level regions. Future work should explore the relationship between fMRI acquisition TR and fingerprinting by employing a sliding windows approach (Van De Ville et al. 2021) or other models assessing dynamic FC (Keilholz et al. 2017; Preti, Bolton, and Van De Ville 2017). Finally, our study only evaluates resting-state fMRI data. Applying the same framework to task-based data could provide interesting insights on whether functional connectomes derived by different TR acquisitions can explain different cognitive dimensions (Sareen et al. 2021). In fact, it has been proven that the temporal scales of fingerprinting can be linked to behavior, with faster time scales more related to, for instance, multisensory stimulation and visuospatial attention, and slower time scales more related, for example, to language, social cognition and working memory (Van De Ville et al. 2021). Following this rationale, subject identifiability might be more or less successfully achieved according to the different tasks subjects perform in the MRI scanner (Amico and Goñi 2018; Finn et al. 2015; Van de Ville et al. 2021), and to the protocols' TR.

5 | Conclusion

This study demonstrates the robustness and reliability of FC fingerprinting derived from rs-fMRI across a wide range of TRs, including "fast" (TR 0.5 s) and "slow" (TR 3 s) full brain coverage, with intermediate values within the same group of healthy volunteers. Interestingly, while always high, subject identifiability was influenced by the TR. In fact, our work shows that the fastest and slowest TRs improved identifiability relative to the other intermediate TRs, which is consistent with a relatively lower contribution of physiological noise. The study also confirms that FC fingerprints have different timescales across the brain. In particular, high-level associative areas being more stable across protocols with different TRs, contributed more to subject identifiability. Instead, low-level sensorimotor networks were mostly responsible for differentiating subjects between different TR acquisitions. Overall, these findings suggest that pooling rs-fMRI data for large-sample fingerprinting analyses is feasible, but TR differences should be taken into consideration to reduce identifiability biases and to understand the contribution of different functional networks to the fingerprints and related biomarkers.

Acknowledgements

The authors would like to thank three anonymous reviewers for all valuable comments and suggestions, which helped to improve the quality of the manuscript. This study was supported by the Autonomous Province of Trento, Italy (Project: "NeuSurPlan and integrated approach to neurosurgery planning based on multimodal data"), the ISMRM Exchange Award 2021–2022 ("Investigating in-vivo human brain dynamic connectivity with fast fMRI"), the Dipartimento di Eccellenza project 2018–2022 (Italian Ministry of Education, University and Research), and the Municipality of the City of Rovereto, Trento, Italy (Project: "Advanced neuroimaging to study aging"). EA acknowledges financial support from the SNSF Ambizione project "Fingerprinting the brain: network science to extract features of cognition, behavior and dysfunction" (grant number PZ00P2_185716). Open access publishing facilitated by Universita degli Studi di Trento, as part of the Wiley - CRUI-CARE agreement.

Ethics Statement

All volunteers gave written informed consent to participate in this study, which was approved by the Ethical Committee of the University of Trento, Italy, and conforms to the recognized standards of the Declaration of Helsinki.

Conflicts of Interest

The authors declare no conflicts of interest.

Data Availability Statement

For privacy reasons, the dataset used for the current study cannot be shared. Upon acceptance, the code used for performing the analysis described in the present paper will be make publicly available through GitHub (https://github.com/CIMeC-MRI-Lab).

References

Ahrends, C., A. Stevner, U. Pervaiz, et al. 2022. "Data and Model Considerations for Estimating Time-Varying Functional Connectivity in fMRI." *NeuroImage* 252: 119026. https://doi.org/10.1016/j.neuroimage.2022.119026.

Akin, B., H. L. Lee, J. Hennig, and P. LeVan. 2017. "Enhanced Subject-Specific Resting-State Network Detection and Extraction With Fast fMRI." *Human Brain Mapping* 38, no. 2: 817–830. https://doi.org/10.1002/hbm.23420.

Alexander-Bloch, A. F., H. Shou, S. Liu, et al. 2018. "On Testing for Spatial Correspondence Between Maps of Human Brain Structure and Function." *NeuroImage* 178: 540–551. https://doi.org/10.1016/j.neuroimage.2018.05.070.

Amico, E., and J. Goñi. 2018. "The Quest for Identifiability in Human Functional Connectomes." *Scientific Reports* 8, no. 1: 8254. https://doi.org/10.1038/s41598-018-25089-1.

Anderson, J. S., M. A. Ferguson, M. Lopez-Larson, and D. Yurgelun-Todd. 2011. "Reproducibility of Single-Subject Functional Connectivity Measurements." *American Journal of Neuroradiology* 32, no. 3: 548–555. https://doi.org/10.3174/ajnr.A2330.

Bari, S., E. Amico, N. Vike, T. M. Talavage, and J. Goñi. 2019. "Uncovering Multi-Site Identifiability Based on Resting-State Functional Connectomes." *NeuroImage* 202: 115967. https://doi.org/10.1016/j.neuroimage.2019.06.045.

Barth, M., F. Breuer, P. J. Koopmans, D. G. Norris, and B. A. Poser. 2016. "Simultaneous Multislice (SMS)I Techniques." *Magnetic Resonance in Medicine* 75, no. 1: 63–81. https://doi.org/10.1002/mrm.25897.

Bartko, J. J. 1966. "The Intraclass Correlation Coefficient as a Measure of Reliability." *Psychological Reports* 19, no. 1: 3–11. https://doi.org/10.2466/pr0.1966.19.1.3.

Begley, C. G., and J. P. A. Ioannidis. 2015. "Reproducibility in Science: Improving the Standard for Basic and Preclinical Research." *Circulation Research* 116, no. 1: 116–126. https://doi.org/10.1161/CIRCRESAHA.114.303819.

Binder, J. R., R. H. Desai, W. W. Graves, and L. L. Conant. 2009. "Where Is the Semantic System? A Critical Review and Meta-Analysis of 120 Functional Neuroimaging Studies." *Cerebral Cortex* 19, no. 12: 2767–2796. https://doi.org/10.1093/cercor/bhp055.

Birn, R. M., E. K. Molloy, R. Patriat, et al. 2013. "The Effect of Scan Length on the Reliability of Resting-State fMRI Connectivity Estimates." *NeuroImage* 83: 550–558. https://doi.org/10.1016/j.neuroimage.2013.05.099.

Bonetto, G., Y. Kamen, K. A. Evans, and R. T. Káradóttir. 2020. "Unraveling Myelin Plasticity." *Frontiers in Cellular Neuroscience* 14: 156. https://doi.org/10.3389/fncel.2020.00156.

Boubela, R., K. Kalcher, C. Nasel, and E. Moser. 2014. "Scanning Fast and Slow: Current Limitations of 3 Tesla Functional MRI and Future Potential." *Frontiers in Physics* 2: 00001. https://doi.org/10.3389/fphy.2014.00001.

Caballero-Gaudes, C., and R. C. Reynolds. 2017. "Methods for Cleaning the BOLD fMRI Signal." *NeuroImage* 154: 128–149. https://doi.org/10.1016/j.neuroimage.2016.12.018.

Castellanos, F. X., A. Di Martino, R. C. Craddock, A. D. Mehta, and M. P. Milham. 2013. "Clinical Applications of the Functional Connectome." *NeuroImage* 80: 527–540. https://doi.org/10.1016/j.neuroimage.2013.04.083.

Choe, A. S., C. K. Jones, S. E. Joel, et al. 2015. "Reproducibility and Temporal Structure in Weekly Resting-State fMRI Over a Period of 3.5 Years." *PLoS One* 10, no. 10: e0140134. https://doi.org/10.1371/journal.pone.0140134.

Cicchetti, D. V., and S. A. Sparrow. 1981. "Developing Criteria for Establishing Interrater Reliability of Specific Items: Applications to Assessment of Adaptive Behavior." *American Journal of Mental Deficiency* 86, no. 2: 127–137.

Cioli, C., H. Abdi, D. Beaton, Y. Burnod, and S. Mesmoudi. 2014. "Differences in Human Cortical Gene Expression Match the Temporal Properties of Large-Scale Functional Networks." *PLoS One* 9, no. 12: e115913. https://doi.org/10.1371/journal.pone.0115913.

Corbin, N., N. Todd, K. J. Friston, and M. F. Callaghan. 2018. "Accurate Modeling of Temporal Correlations in Rapidly Sampled fMRI Time Series." *Human Brain Mapping* 39, no. 10: 3884–3897. https://doi.org/10.1002/hbm.24218.

Cordes, D., V. M. Haughton, K. Arfanakis, et al. 2001. "Frequencies Contributing to Functional Connectivity in the Cerebral Cortex in "Resting-State" Data." *American Journal of Neuroradiology* 22, no. 7: 1326–1333.

Crews, F., J. He, and C. Hodge. 2007. "Adolescent Cortical Development: A Critical Period of Vulnerability for Addiction." *Pharmacology Biochemistry and Behavior* 86, no. 2: 189–199. https://doi.org/10.1016/j.pbb.2006.12.001.

Damoiseaux, J. S., S. A. R. B. Rombouts, F. Barkhof, et al. 2006. "Consistent Resting-State Networks Across Healthy Subjects." *Proceedings of the National Academy of Sciences of the United States of America* 103, no. 37: 13848–13853. https://doi.org/10.1073/pnas.0601417103.

Dowdle, L. T., G. Ghose, C. C. Chen, K. Ugurbil, E. Yacoub, and L. Vizioli. 2021. "Statistical Power or More Precise Insights Into Neuro-Temporal Dynamics? Assessing the Benefits of Rapid Temporal Sampling in fMRI." *Progress in Neurobiology* 207: 102171. https://doi.org/10.1016/j.pneurobio.2021.102171.

Dufford, A. J., S. Noble, S. Gao, and D. Scheinost. 2021. "The Instability of Functional Connectomes Across the First Year of Life." *Developmental Cognitive Neuroscience* 51: 101007. https://doi.org/10.1016/j.dcn.2021.101007.

Edelstein, W. A., G. H. Glover, C. J. Hardy, and R. W. Redington. 1986. "The Intrinsic Signal-To-Noise Ratio in NMR Imaging." *Magnetic Resonance in Medicine* 3, no. 4: 604–618. https://doi.org/10.1002/mrm.1910030413.

Feinberg, D. A., S. Moeller, S. M. Smith, et al. 2010. "Multiplexed Echo Planar Imaging for Sub-Second Whole Brain FMRI and Fast Diffusion Imaging." *PLoS One* 5, no. 12: e15710. https://doi.org/10.1371/journal.pone.0015710.

Feinberg, D. A., and K. Setsompop. 2013. "Ultra-Fast MRI of the Human Brain With Simultaneous Multi-Slice Imaging." *Journal of Magnetic Resonance* 229: 90–100. https://doi.org/10.1016/j.jmr.2013.02.002.

Fernandes, B. S., L. M. Williams, J. Steiner, M. Leboyer, A. F. Carvalho, and M. Berk. 2017. "The New Field of 'Precision Psychiatry'." *BMC Medicine* 15, no. 1: 80. https://doi.org/10.1186/s12916-017-0849-x.

Finn, E. S., X. Shen, D. Scheinost, et al. 2015. "Functional Connectome Fingerprinting: Identifying Individuals Using Patterns of Brain Connectivity." *Nature Neuroscience* 18, no. 11: 1664–1671. https://doi.org/10.1038/nn.4135.

Fraschini, M., A. Hillebrand, M. Demuru, L. Didaci, and G. L. Marcialis. 2015. "An EEG-Based Biometric System Using Eigenvector Centrality in Resting State Brain Networks." *IEEE Signal Processing Letters* 22, no. 6: 666–670. https://doi.org/10.1109/LSP.2014.2367091.

Friston, K. J. 1994. "Functional and Effective Connectivity in Neuroimaging: A Synthesis." *Human Brain Mapping* 2, no. 1–2: 56–78. https://doi.org/10.1002/hbm.460020107.

Gao, R., R. L. van den Brink, T. Pfeffer, and B. Voytek. 2020. "Neuronal Timescales Are Functionally Dynamic and Shaped by Cortical Microarchitecture." *eLife* 9: e61277. https://doi.org/10.7554/eLife.61277.

Glasser, M. F., T. S. Coalson, E. C. Robinson, et al. 2016. "A Multi-Modal Parcellation of Human Cerebral Cortex." *Nature* 536, no. 7615: 171–178. https://doi.org/10.1038/nature18933.

Gold, J. I., and M. N. Shadlen. 2007. "The Neural Basis of Decision Making." *Annual Review of Neuroscience* 30, no. 1: 535–574. https://doi.org/10.1146/annurev.neuro.29.051605.113038.

Gordon, E. M., T. O. Laumann, A. W. Gilmore, et al. 2017. "Precision Functional Mapping of Individual Human Brains." *Neuron* 95, no. 4: 791–807. https://doi.org/10.1016/j.neuron.2017.07.011.

Hacker, C. D., A. Z. Snyder, M. Pahwa, M. Corbetta, and E. C. Leuthardt. 2017. "Frequency-Specific Electrophysiologic Correlates of Resting State fMRI Networks." *NeuroImage* 149: 446–457. https://doi.org/10.1016/j.neuroimage.2017.01.054.

Hu, D., F. Wang, H. Zhang, et al. 2022. "Existence of Functional Connectome Fingerprint During Infancy and Its Stability Over Months." *Journal of Neuroscience* 42, no. 3: 377–389. https://doi.org/10.1523/JNEUROSCI.0480-21.2021.

Huntenburg, J. M., P.-L. Bazin, A. Goulas, C. L. Tardif, A. Villringer, and D. S. Margulies. 2017. "A Systematic Relationship Between Functional Connectivity and Intracortical Myelin in the Human Cerebral Cortex." *Cerebral Cortex* 27, no. 2: 981–997. https://doi.org/10.1093/cercor/bhx030.

Huotari, N., L. Raitamaa, H. Helakari, et al. 2019. "Sampling Rate Effects on Resting State fMRI Metrics." *Frontiers in Neuroscience* 13: 279. https://doi.org/10.3389/fnins.2019.00279.

Jahanian, H., S. Holdsworth, T. Christen, et al. 2019. "Advantages of Short Repetition Time Resting-State Functional MRI Enabled by Simultaneous Multi-Slice Imaging." *Journal of Neuroscience Methods* 311: 122–132. https://doi.org/10.1016/j.jneumeth.2018.09.033.

Jenkinson, M., C. F. Beckmann, T. E. J. Behrens, M. W. Woolrich, and S. M. Smith. 2012. "FSL." *NeuroImage* 62, no. 2: 782–790. https://doi.org/10.1016/j.neuroimage.2011.09.015.

Jolliffe, I. 2014. "Principal Component Analysis." In *Wiley StatsRef: Statistics Reference Online*. Chichester, West Sussex, England, UK: John Wiley & Sons, Ltd. https://doi.org/10.1002/9781118445112.stat06472.

Keilholz, S., C. Caballero-Gaudes, P. Bandettini, G. Deco, and V. Calhoun. 2017. "Time-Resolved Resting-State Functional Magnetic Resonance Imaging Analysis: Current Status, Challenges, and New Directions." *Brain Connectivity* 7, no. 8: 465–481. https://doi.org/10.1089/brain.2017.0543.

Kiviniemi, V., X. Wang, V. Korhonen, et al. 2016. "Ultra-Fast Magnetic Resonance Encephalography of Physiological Brain Activity—Glymphatic Pulsation Mechanisms?" *Journal of Cerebral Blood Flow & Metabolism* 36, no. 6: 1033–1045. https://doi.org/10.1177/0271678X15622047.

Laird, A. R., P. M. Fox, S. B. Eickhoff, et al. 2011. "Behavioral Interpretations of Intrinsic Connectivity Networks." *Journal of Cognitive Neuroscience* 23, no. 12: 4022–4037. https://doi.org/10.1162/jocn_a_00077.

Larkman, D. J., J. V. Hajnal, A. H. Herlihy, G. A. Coutts, I. R. Young, and G. Ehnholm. 2001. "Use of Multicoil Arrays for Separation of Signal From Multiple Slices Simultaneously Excited." *Journal of Magnetic Resonance Imaging* 13, no. 2: 313–317. https://doi.org/10.1002/1522-2586(200102)13:2<313::AID-JMRI1045>3.0.CO;2-W.

Laumann, T. O., E. M. Gordon, B. Adeyemo, et al. 2015. "Functional System and Areal Organization of a Highly Sampled Individual Human Brain." *Neuron* 87, no. 3: 657–670. https://doi.org/10.1016/j.neuron.2015.06.037.

Lee, H. L., B. Zahneisen, T. Hugger, P. LeVan, and J. Hennig. 2013b. "Tracking Dynamic Resting-State Networks at Higher Frequencies Using MR-Encephalography." *NeuroImage* 65: 216–222. https://doi.org/10.1016/j.neuroimage.2012.10.015.

Lee, M. H., C. D. Smyser, and J. S. Shimony. 2013a. "Resting-State fMRI: A Review of Methods and Clinical Applications." *American Journal of Neuroradiology* 34, no. 10: 1866–1872. https://doi.org/10.3174/ajnr.A3263.

Liu, T. T. 2016. "Noise Contributions to the fMRI Signal: An Overview." *NeuroImage* 143: 141–151. https://doi.org/10.1016/j.neuroimage.2016.09.008.

Lowe, M. J., B. J. Mock, and J. A. Sorenson. 1998. "Functional Connectivity in Single and Multislice Echoplanar Imaging Using Resting-State Fluctuations." *NeuroImage* 7, no. 2: 119–132. https://doi.org/10.1006/nimg.1997.0315.

Margulies, D. S., S. S. Ghosh, A. Goulas, et al. 2016. "Situating the Default-Mode Network Along a Principal Gradient of Macroscale Cortical Organization." *Proceedings of the National Academy of Sciences of the United State of America* 113, no. 44: 12574–12579. https://doi.org/10.1073/pnas.1608282113.

McGraw, K., and S. P. Wong. 1996. "Forming Inferences About Some Intraclass Correlation Coefficients." *Psychological Methods* 1: 30–46. https://doi.org/10.1037/1082-989X.1.1.30.

Mesmoudi, S., V. Perlbarg, D. Rudrauf, et al. 2013. "Resting State Networks' Corticotopy: The Dual Intertwined Rings Architecture." *PLoS One* 8, no. 7: e67444. https://doi.org/10.1371/journal.pone.0067444.

Mueller, S., D. Wang, M. D. Fox, et al. 2015. "Reliability Correction for Functional Connectivity: Theory and Implementation." *Human Brain Mapping* 36, no. 11: 4664–4680. https://doi.org/10.1002/hbm.22947.

Nichols, T. E., and A. P. Holmes. 2002. "Nonparametric Permutation Tests for Functional Neuroimaging: A Primer With Examples." *Human Brain Mapping* 15, no. 1: 1–25. https://doi.org/10.1002/hbm.1058.

Noble, S., M. N. Spann, F. Tokoglu, X. Shen, R. T. Constable, and D. Scheinost. 2017. "Influences on the Test-Retest Reliability of Functional Connectivity MRI and Its Relationship With Behavioral Utility." *Cerebral Cortex* 27, no. 11: 5415–5429. https://doi.org/10.1093/cercor/bhx230.

Özbay, P. S., C. Chang, D. Picchioni, et al. 2019. "Sympathetic Activity Contributes to the fMRI Signal." *Communications Biology* 2, no. 1: Article 1. https://doi.org/10.1038/s42003-019-0659-0.

Pervaiz, U., D. Vidaurre, M. W. Woolrich, and S. M. Smith. 2020. "Optimising Network Modelling Methods for fMRI." *NeuroImage* 211: 116604. https://doi.org/10.1016/j.neuroimage.2020.116604.

Polimeni, J. R., and L. D. Lewis. 2021. "Imaging Faster Neural Dynamics With Fast fMRI: A Need for Updated Models of the Hemodynamic Response." *Progress in Neurobiology* 207: 102174. https://doi.org/10.1016/j.pneurobio.2021.102174.

Posse, S., E. Ackley, R. Mutihac, et al. 2012. "Enhancement of Temporal Resolution and BOLD Sensitivity in Real-Time fMRI Using Multi-Slab Echo-Volumar Imaging." *NeuroImage* 61, no. 1: 115–130. https://doi.org/10.1016/j.neuroimage.2012.02.059.

Preibisch, C., J. Gabriel Castrillón G, M. Bührer, and V. Riedl. 2015. "Evaluation of Multiband EPI Acquisitions for Resting State fMRI." *PLoS One* 10, no. 9: e0136961. https://doi.org/10.1371/journal.pone.0136961.

Preti, M. G., T. A. Bolton, and D. Van De Ville. 2017. "The Dynamic Functional Connectome: State-of-the-Art and Perspectives." *NeuroImage* 160: 41–54. https://doi.org/10.1016/j.neuroimage.2016.12.061.

Preti, M. G., and D. Van De Ville. 2019. "Decoupling of Brain Function From Structure Reveals Regional Behavioral Specialization in Humans." *Nature Communications* 10, no. 1: 10. https://doi.org/10.1038/s41467-019-12765-7.

Rajapandian, M., E. Amico, K. Abbas, M. Ventresca, and J. Goñi. 2020. "Uncovering Differential Identifiability in Network Properties of Human Brain Functional Connectomes." *Network Neuroscience* 4, no. 3: 698–713. https://doi.org/10.1162/netn_a_00140.

Reynaud, O., J. Jorge, R. Gruetter, J. P. Marques, and W. van der Zwaag. 2017. "Influence of Physiological Noise on Accelerated 2D and 3D Resting State Functional MRI Data at 7T." *Magnetic Resonance in Medicine* 78, no. 3: 888–896. https://doi.org/10.1002/mrm.26823.

Rocca, D. L., P. Campisi, B. Vegso, et al. 2014. "Human Brain Distinctiveness Based on EEG Spectral Coherence Connectivity." *IEEE Transactions on Biomedical Engineering* 61, no. 9: 2406–2412. https://doi.org/10.1109/TBME.2014.2317881.

Romano, A., E. Trosi Lopez, M. Liparoti, et al. 2022. "The Progressive Loss of Brain Network Fingerprints in Amyotrophic Lateral Sclerosis Predicts Clinical Impairment." *NeuroImage: Clinical* 35: 103095. https://doi.org/10.1016/j.nicl.2022.103095.

Runyan, C. A., E. Piasini, S. Panzeri, and C. D. Harvey. 2017. "Distinct Timescales of Population Coding Across Cortex." *Nature* 548, no. 7665: 92–96. https://doi.org/10.1038/nature23020.

Sarafyazd, M., and M. Jazayeri. 2019. "Hierarchical Reasoning by Neural Circuits in the Frontal Cortex." *Science* 364, no. 6441: eaav8911. https://doi.org/10.1126/science.aav8911.

Sarar, G., B. Rao, and T. Liu. 2021. "Functional Connectome Fingerprinting Using Shallow Feedforward Neural Networks." *Proceedings of the National Academy of Sciences of the United States of America* 118, no. 15: e2021852118. https://doi.org/10.1073/pnas.2021852118.

Sareen, E., S. Zahar, D. V. D. Ville, A. Gupta, A. Griffa, and E. Amico. 2021. "Exploring MEG Brain Fingerprints: Evaluation, Pitfalls, and Interpretations." *NeuroImage* 240: 118331. https://doi.org/10.1016/j.neuroimage.2021.118331.

Saviola, F., S. Tambalo, D. Gift-Cabalo, et al. 2022. "Head Motion Correction Shapes Functional Network Estimates: Evidence From Healthy and Parkinson's Disease Cohorts." *bioRxiv*: 2022.12.26.520413. https://doi.org/10.1101/2022.12.26.520413.

Schaefer, A., R. Kong, E. M. Gordon, et al. 2018. "Local-Global Parcellation of the Human Cerebral Cortex From Intrinsic Functional Connectivity MRI." *Cerebral Cortex* 28, no. 9: 3095–3114. https://doi.org/10.1093/cercor/bhx179.

Shah, L. M., J. A. Cramer, M. A. Ferguson, R. M. Birn, and J. S. Anderson. 2016. "Reliability and Reproducibility of Individual Differences in Functional Connectivity Acquired During Task and Resting State." *Brain and Behavior: A Cognitive Neuroscience Perspective* 6, no. 5: e00456. https://doi.org/10.1002/brb3.456.

Shehzad, Z., A. M. C. Kelly, P. T. Reiss, et al. 2009. "The Resting Brain: Unconstrained Yet Reliable." *Cerebral Cortex* 19, no. 10: 2209–2229. https://doi.org/10.1093/cercor/bhn256.

Smith, S. M., C. F. Beckmann, J. Andersson, et al. 2013. "Resting-State fMRI in the Human Connectome Project." *NeuroImage* 80: 144–168. https://doi.org/10.1016/j.neuroimage.2013.05.039.

Smith, S. M., T. E. Nichols, D. Vidaurre, et al. 2015. "A Positive-Negative Mode of Population Covariation Links Brain Connectivity, Demographics and Behavior." *Nature Neuroscience* 18, no. 11: 1567. https://doi.org/10.1038/nn.4125.

Smitha, K. A., K. Akhil Raja, K. M. Arun, et al. 2017. "Resting State fMRI: A Review on Methods in Resting State Connectivity Analysis and Resting State Networks." *Neuroradiology Journal* 30, no. 4: 305–317. https://doi.org/10.1177/1971400917697342.

Sorrentino, P., R. Rucco, A. Lardone, et al. 2021. "Clinical Connectome Fingerprints of Cognitive Decline." *NeuroImage* 238: 118253. https://doi.org/10.1016/j.neuroimage.2021.118253.

St-Onge, F., M. Javanray, A. Pichet Binette, et al. 2023. "Functional Connectome Fingerprinting Across the Lifespan." *Network Neuroscience* 7, no. 3: 1206–1227. https://doi.org/10.1162/netn_a_00320.

Svaldi, D. O., J. Goñi, K. Abbas, et al. 2021. "Optimizing Differential Identifiability Improves Connectome Predictive Modeling of Cognitive Deficits From Functional Connectivity in Alzheimer's Disease." *Human Brain Mapping* 42, no. 11: 3500–3516. https://doi.org/10.1002/hbm.25448.

Tomasi, D. G., E. Shokri-Kojori, and N. D. Volkow. 2017. "Temporal Evolution of Brain Functional Connectivity Metrics: Could 7 min of Rest Be Enough?" *Cerebral Cortex* 27, no. 8: 4153–4165. https://doi.org/10.1093/cercor/bhw227.

Troisi Lopez, E., R. Minino, M. Liparoti, et al. 2023. "Fading of Brain Network Fingerprint in Parkinson's Disease Predicts Motor Clinical Impairment." *Human Brain Mapping* 44, no. 3: 1239–1250. https://doi.org/10.1002/hbm.26156.

Van De Ville, D., Y. Farouj, M. G. Preti, R. Liégeois, and E. Amico. 2021. "When Makes You Unique: Temporality of the Human Brain Fingerprint." *Science Advances* 7, no. 42: eabj0751. https://doi.org/10.1126/sciadv.abj0751.

Van Dijk, K. R. A., T. Hedden, A. Venkataraman, K. C. Evans, S. W. Lazar, and R. L. Buckner. 2010. "Intrinsic Functional Connectivity as a Tool for Human Connectomics: Theory, Properties, and Optimization." *Journal of Neurophysiology* 103, no. 1: 297–321. https://doi.org/10.1152/jn.00783.2009.

Van Essen, D. C., S. M. Smith, D. M. Barch, T. E. J. Behrens, E. Yacoub, and K. Ugurbil. 2013. "The WU-Minn Human Connectome Project: An Overview." *NeuroImage* 80: 62–79. https://doi.org/10.1016/j.neuroimage.2013.05.041.

Vidaurre, D., S. M. Smith, and M. W. Woolrich. 2017. "Brain Network Dynamics Are Hierarchically Organized in Time." *Proceedings of the National Academy of Sciences of the United States of America* 114, no. 48: 12827–12832. https://doi.org/10.1073/pnas.1705120114.

Wang, Y., W. Hinds, C. S. Duarte, et al. 2021. "Intra-Session Test-Retest Reliability of Functional Connectivity in Infants." *NeuroImage* 239: 118284. https://doi.org/10.1016/j.neuroimage.2021.118284.

Xu, X., I. L. Hanganu-Opatz, and M. Bieler. 2020. "Cross-Talk of Low-Level Sensory and High-Level Cognitive Processing: Development, Mechanisms, and Relevance for Cross-Modal Abilities of the Brain." *Frontiers in Neurorobotics* 14: 7. https://doi.org/10.3389/fnbot.2020.00007.

Yang, Z., and L. D. Lewis. 2021. "Imaging the Temporal Dynamics of Brain States With Highly Sampled fMRI." *Current Opinion in Behavioral Sciences* 40: 87–95. https://doi.org/10.1016/j.cobeha.2021.02.005.

Yeo, B. T. T., F. M. Krienen, J. Sepulcre, et al. 2011. "The Organization of the Human Cerebral Cortex Estimated by Intrinsic Functional Connectivity." *Journal of Neurophysiology* 106, no. 3: 1125–1165. https://doi.org/10.1152/jn.00338.2011.

Zalesky, A., A. Fornito, L. Cocchi, L. L. Gollo, and M. Breakspear. 2014. "Time-Resolved Resting-State Brain Networks." *Proceedings of the National Academy of Sciences of the United States of America* 111, no. 28: 10341–10346. https://doi.org/10.1073/pnas.1400181111.

Zylberberg, J., and B. W. Strowbridge. 2017. "Mechanisms of Persistent Activity in Cortical Circuits: Possible Neural Substrates for Working Memory." *Annual Review of Neuroscience* 40, no. 1: 603–627. https://doi.org/10.1146/annurev-neuro-070815-014006.

Supporting Information

Additional supporting information can be found online in the Supporting Information section.